Europe PMC Funders Group
Author Manuscript
Nat Immunol. Author manuscript; available in PMC 2015 February 01.

Published in final edited form as:
Nat Immunol. 2014 August ; 15(8): 749–757. doi:10.1038/ni.2936.

The metabolic checkpoint kinase mTOR is essential for interleukin-15 signaling during NK cell development and activation

Antoine Marçais[1,2,3,4,5], **Julien Cherfils-Vicini**[#6], **Charlotte Viant**[#7], **Sophie Degouve**[1,2,3,4,5], **Sébastien Viel**[1,2,3,4,5,8], **Aurore Fenis**[7], **Jessica Rabilloud**[1,2,3,4,5], **Katia Mayol**[1,2,3,4,5], **Armelle Tavares**[1,2,3,4,5], **Jacques Bienvenu**[8], **Yann-Gaël Gangloff**[3,9], **Eric Gilson**[6,10], **Eric Vivier**[7], and **Thierry Walzer**[1,2,3,4,5]

[1]CIRI, Centre International de Recherche en Infectiologie - International Center for Infectiology Research, Lyon, France

[2]Inserm, U1111, Lyon, France

[3]Ecole Normale Supérieure de Lyon, Lyon, France

[4]Université Lyon 1, Lyon, France

[5]CNRS, UMR5308, Lyon, France

[6]Institute for Research on Cancer and Aging, Nice (IRCAN), Nice University, CNRS UMR7284/ INSERM U1081, Faculty of Medicine, Nice 06107, France

[7]Centre d'Immunologie de Marseille-Luminy, INSERM U1104; CNRS UMR7280; Aix Marseille Université, UM2, Marseille, France

[8]Laboratoire d'Immunologie, Hospices Civils de Lyon, Centre Hospitalier Lyon Sud, France

[9]LBMC; CNRS, UMR 5239, Lyon, France

[10]Department of Medical Genetics, Archet 2 Hospital, CHU of Nice, BP 3079, 06202 Nice cedex 3, France

[#] These authors contributed equally to this work.

Abstract

Interleukin-15 (IL-15) controls both the homeostasis and the peripheral activation of Natural Killer (NK) cells. The molecular basis for this duality of action remains unknown. Here we report that the metabolic checkpoint kinase mTOR is activated and boosts bioenergetic metabolism upon NK cell exposure to high concentrations of IL-15 whereas low doses of IL-15 only triggers the phosphorylation of the transcription factor STAT5. mTOR stimulates NK cell growth and nutrient

Users may view, print, copy, and download text and data-mine the content in such documents, for the purposes of academic research, subject always to the full Conditions of use:http://www.nature.com/authors/editorial_policies/license.html#terms

Corresponding author: Thierry Walzer, Centre International de Recherche en Infectiologie (CIRI), INSERM U1111, 21 Avenue Tony Garnier - 69365 LYON cedex 07, France, Tel +33 (0)437 28 23 73., Thierry.walzer@inserm.fr.

COMPETING FINANCIAL INTERESTS
The authors declare no competing financial interests.

Europe PMC Funders Author Manuscripts
Europe PMC Funders Author Manuscripts

Europe PMC Funders Author Manuscripts

Europe PMC Funders Author Manuscripts

uptake and positively feeds back onto the IL-15 receptor. This process is essential to sustain NK cell proliferation during development and acquisition of cytolytic potential upon inflammation or virus infection. The mTORC1 inhibitor rapamycin inhibits NK cell cytotoxicity both in mouse and human, which likely contribute to the immunosuppressant activities of this drug in different clinical settings.

Natural killer (NK) cells are Innate Lymphoid Cells (ILC) involved in the immuno-surveillance of cancers and in the early control of infections by intracellular pathogens [1]. They can kill cells recognized as targets through a battery of surface receptors and produce large amounts of interferon-γ (IFN-γ) upon activation [1]. The growing ILC family has been reclassified into 3 groups according to the pattern of cytokine they secrete. In this classification, NK cells are part of the group 1 ILC subset [2]. They express the NKp46 activating receptor [3], a characteristic they share with the interleukin-22-(IL-22) producing subset ILC3 involved in gut innate immunity[4-6]. In mice, NK cells mainly develop in the BM. Sequential developmental intermediates, from immature to mature, can be defined on the basis of surface expression of the tumor necrosis factor (TNF) superfamily member CD27 and the integrin CD11b: $CD11b^{lo}CD27^{hi}$ NK cells (hereafter referred to as "$CD11b^{lo}$"), $CD11b^{hi}CD27^{hi}$ (double positive or "DP"), and $CD11b^{hi}CD27^{lo}$ ("$CD27^{lo}$") [7,8]. Upon disruption of IL-15 signaling, NK cell survival is drastically reduced and the development of the remaining cells is arrested at the $CD11b^{lo}$ immature stage, demonstrating a non-redundant role of this cytokine in NK cell homeostasis and differentiation [9-12]. IL-15 trans-presentation by Toll-like receptor ligand-activated dendritic cells (DCs) also controls acquisition of NK cell effector functions [13]. How a single cytokine can display homeostatic as well as inflammatory effects remains a challenging question. It was suggested that different quantities of IL-15 signaling induce graded responses on NK cells and could thus explain its functional duality [14-16]. However, the link between IL-15 functional effects and signaling pathways activated following IL-15 ligation is poorly characterized. Deletion of the transcription factor STAT5 in NK cells, suggests that IL-15 mediates its pro-survival effects through this pathway [17]. Whether STAT5 is sufficient to induce NK cell proliferation and up regulate their cytotoxic potential is however unknown.

The link between metabolic regulation and immune cell activation has received considerable attention [18]. Following antigenic challenge T cells upregulate their metabolism to face the biosynthetic demand resulting in a change from a quiescent to a proliferative state. Conversely, the resolution of the response is accompanied by a shift of the T cells back to a quiescent state. Metabolic regulation is also coupled to acquisition of effector functions [19] and a migratory pattern of effector cells [20]. A central player integrating various metabolic, antigenic and inflammatory cues is the evolutionarily conserved Ser/Thr kinase mechanistic Target Of Rapamycin (mTOR) [21]. mTOR takes part in two distinct complexes termed mTORC1 and mTORC2. mTORC1 controls translation mainly through the phosphorylation of eIF4E binding protein 1 (4EBP1) and S6 ribosomal kinase (S6K). S6K then phosphorylates S6 ribosomal protein and mTOR itself on Ser2448 [22]. Moreover, mTORC1 also takes part in the control of glycolysis by promoting the transcription factors HIF-1α and Myc expression as well as upregulating nutrient transporter expression, in the control of lipid synthesis by activating SREBP and in the control of autophagy. mTORC2 is known to

Europe PMC Funders Author Manuscripts

Europe PMC Funders Author Manuscripts

phosphorylate Akt on Ser473, which completes activation initiated by phosphorylation on Thr308 deposited by Phosphoinositide Dependent Kinase 1 (PDK1) and allows nuclear export of the Foxo transcription factors family. mTORC2 also controls cytoskeletal organization. Moreover, mTOR phosphorylates itself on Ser2481. Many recent studies have explored the role of mTOR and downstream effectors in T cell differentiation [23]. By contrast, there is a dearth of information on NK cell metabolic regulation and the role of mTOR in their physiology.

We thus set out to characterize the basic NK cell metabolic needs and how they are linked to differentiation and priming following IL-15 stimulation. We found that, as NK cells mature, they progress to quiescence. This state can be reversed upon virus or cytokine stimulation. These changes are controlled by the mTOR, the deletion of which reveals its critical non-redundant role in the regulation of two key checkpoints of NK cell biology: proliferation in the BM and activation in the periphery. Moreover, mTOR is an essential component of IL-15 signaling, activated upon NK cell exposure to high IL-15 concentrations.

Results

Development and activation regulate NK cell metabolism

We monitored metabolic changes during NK cell differentiation and activation. We detected a significant contraction of cell size and granularity as the cells terminally differentiated (Supplementary Fig. 1a). Conversely, following *in vitro* treatment with IL-15 (Supplementary Fig. 1b), activation by injection of the TLR3 and RIG-I ligand poly(I:C) *in vivo* (Supplementary Fig. 1c) or following influenza A/WSN/33 H1N1 infection (Supplementary Fig. 1d), peripheral NK cell size and granularity increased substantially. In metazoans, a cell's ability to access nutrients depends on expression of dedicated transporters [18]. Expression of CD71 the transferrin receptor and CD98 the heavy chain of the System L amino-acid transporter as well as glucose uptake estimated by measure of the 2-NBDG uptake decreased by 2-3 fold following the DP to $CD27^{lo}$ transition in the BM (Fig. 1a). In the spleen, these markers are expressed at lower level, but their expression also decreases upon differentiation (Fig. 1a). *In vivo* activation following poly(I:C) injection resulted in a clear increase in CD98 and CD71 expression as well as glucose uptake in splenic NK cells (Fig. 1b).

To gain a more precise view on metabolic changes occurring during differentiation we searched for unique gene expression signatures differing between $CD11b^{lo}$ and $CD27^{lo}$ NK cells using previously generated microarrays of these subsets [7] and the GSEA software (Supplementary Table 1). Pathways associated with cell growth (Cell cycle, Ribosome) were down regulated in the $CD27^{lo}$ subset. On the contrary pathways associated with the development of a quiescent state (Aerobic sugar or Fatty acid catabolism, Autophagy) were up regulated in the $CD27^{lo}$ subset. Importantly, several negative regulators of the mTOR signaling pathway were enriched in the $CD27^{lo}$ subset (data not shown).

A similar analysis was undertaken to uncover the metabolic regulation associated with NK cell activation. We used datasets generated on NK cells activated 1.5 days following mouse cytomegalovirus (MCMV) infection [24] or 24h *in vitro* activation with IL-15 [25]. The

Europe PMC Funders Author Manuscripts

Europe PMC Funders Author Manuscripts

metabolic terms elicited by MCMV are all also induced by IL-15 treatment (Supplementary Table 2). Activated NK cells displayed higher expression of terms associated with the cell cycle, protein, lipid biosynthesis and carbohydrate catabolism consistent with the observed increase in cell growth and proliferation (Supplementary Figure 1b, c and d and data not shown).

To further characterize NK cell metabolic activity, we took advantage of the Seahorse technology to analyze the O_2 Consumption Rate (OCR) and Extra Cellular Acidification Rate (ECAR), which are proportional to oxidative phosphorylation (OXPHOS) and aerobic glycolysis respectively. Basal metabolism of splenic NK cells was very low for both parameters (Fig. 1c and d). However, IL-15 stimulation enhanced splenic NK cell metabolism, dramatically increasing the basal OXPHOS and aerobic glycolysis (as revealed by glucose addition). Addition of the drug FCCP to unmask potential Spare Respiratory Capacity (SRC) revealed that stimulated NK cells were already developing their maximal respiratory activity. Similarly, the glycolytic reserve (difference between ECAR after glucose injection and ECAR after Oligomycin injection) is close to zero, implying that the maximal glycolytic activity was already reached. Taken together, these data show that splenic NK cell basal metabolism is very low but inducible by IL-15 stimulation.

mTOR regulation upon differentiation and activation

The observation of metabolic changes during NK cell differentiation prompted us to assess the phosphorylation status of mTOR targets. We analyzed the phosphorylation status of mTOR itself (Ser2448 and Ser2481), of mTORC1 downstream targets (4EBP1 Thr37/46 and S6 Ser235/236) and of an mTORC2 target (Akt Ser473). In parallel, the phosphorylation status of STAT5 by Jak3 on Tyr694 downstream of the IL-15 receptor and the phosphorylation of Akt Thr308 added by PDK1 were assessed. We first measured the phosphorylation status of these proteins in bone marrow (BM) and splenic NK cells at steady state and correlated it to the expression of CD11b and CD27. Phosphorylation decreased in a coordinated fashion as the cells matured indicative of a progressive shutdown in mTOR activity both in the BM and in the Spleen (Fig. 2a). A similar pattern was observed for pSTAT5. In contrast, pAkt T308 only decreased in the BM. A direct comparison of the phosphorylation in BM and in splenic NK cells showed that pAkt S473, pmTOR S2448 and pmTOR S2481 were significantly higher on BM NK cells, especially for the $CD11b^{lo}$ subset (Supplementary Fig. 2). We then set out to measure phosphorylation events induced *in vivo* after poly(I:C) stimulation. The extent of the different phosphorylations was upregulated in a coordinated fashion indicating an overall increase in the activity of the pathway (Fig. 2b). As expected since poly(I:C) injection increases IL-15 availability, pSTAT5 was significantly upregulated. In contrast, phosphorylation of Akt on Thr308, dependent on PI3K activity through PDK1 was not significantly changed. Altogether, these results demonstrate that mTOR activity is under the control of developmental and inflammatory signals in NK cells. Moreover, there is a tight parallel between NK cell metabolic status and mTOR activity.

mTOR activity is primarily under IL-15 control

To identify the signals able to regulate mTOR activity in NK cells, we submitted splenic NK cells to a wide range of stimuli for 1 hour *in vitro*. Among all the signals tested, IL-15 was

Europe PMC Funders Author Manuscripts

Europe PMC Funders Author Manuscripts

the only one to elicit a strong increase in pS6 (Fig. 3a). In particular, no effect on pS6 was observed after NK cell receptor triggering. Faint but reproducible effects were also seen upon IL-18 exposure, alone or in combination with IL-12. To better characterize the response to IL-15, we exposed splenocytes for 1 hour to increasing concentrations of this cytokine. We measured in parallel S6 and STAT5 phosphorylation. Higher amounts of IL-15 were needed to activate mTOR (EC50 of 1.5 and 5.3 ng/ml for pSTAT5 and pS6 respectively, Fig. 3b).

To determine whether IL-15 signaling is necessary *in vivo* to maintain physiological mTOR activity, we treated wild-type mice with a F(ab)'2 fragment blocking signaling through CD122. Anti-CD122 treatment led to a rapid reduction of the steady state phosphorylation of S6 in BM NK cells (Fig. 3c, left panel). An overall decrease in the activity of the pathway was confirmed by analysis of other phosphorylations (Fig. 3c right panel). As expected, similar results were obtained for pSTAT5.

To test if the increased IL-15 bioavailability consequent to poly(I:C) injection was responsible for the increased mTOR activity, we co-injected blocking anti-CD122 antibody with poly(I:C). Phosphorylations were measured in splenic NK cells 4 hours later. The increase in pSTAT5 was completely abrogated, indicating a complete inhibition of the IL-15 signaling (Fig. 2b). pAkt and pS6 increase were also significantly dampened by the antibody treatment (Fig. 2b). However, p4EBP1 was not affected suggesting that other signals in vivo can compensate for the absence of IL-15 (Fig. 2b).

Overall, these results show that IL-15 is sufficient to activate mTOR in NK cells. It is also necessary to maintain steady-state activity during NK cell development. Finally, this cytokine is a major but non-exclusive extracellular signal leading to mTOR hyper-activation in an inflammatory context.

mTOR controls NK cell maturation and numbers

To establish the physiological relevance of mTOR signaling in NK cells, we deleted mTOR in NK cells by crossing *Mtor*$^{lox/lox}$ mice [26] with *NKp46*^{ICre} mice [27]. Mice resulting from this cross and their NK cells will hereafter be referred to as NK-*Mtor*$^{-/-}$. We analyzed the consequences of the deletion in NK cells present in various organs (Supplementary Fig. 3). We confirmed that mTOR was indeed absent in NK cells of *NKp46*^{ICre}Mtor$^{lox/lox}$ mice but present at normal amounts in surrounding T cells (Supplementary Fig. 4a). In addition, NK cell size was also decreased and phosphorylation of mTOR targets was consistently reduced (Supplementary Fig. 4b and c) demonstrating that mTOR was functionally absent. Despite this fact, the percentage and number of BM NK cells were normal (Fig. 4a). In stark contrast, NK cells almost disappeared from peripheral organs (Fig. 4a, Supplementary Fig. 4d). Phenotyping of the remaining NK cells revealed a severe block of differentiation in the BM at the CD11b^{lo} to DP stage (Fig. 4b and Supplementary Fig. 5a). This resulted in a complete shift in the distribution among the different NK subsets in the spleen (Fig. 4b and Supplementary Fig. 5a). Consistent with this observation, the expression of the maturation and senescence marker KLRG1 virtually disappeared on NK-*Mtor*$^{-/-}$ NK cells (Fig. 4c).

Europe PMC Funders Author Manuscripts

Europe PMC Funders Author Manuscripts

Next, we conducted a broad phenotypic analysis of splenic *NKp46*^{ICre} (NK-*Mtor*$^{WT/WT}$) vs NK-*Mtor*$^{-/-}$ NK cells (Fig. 4d). To compensate for the differentiation bias occurring in mTOR absence, we focused our analysis on the CD11b^{lo} subset. Markers like CXCR4, CD127 and NK1.1 were up regulated on splenic NK-*Mtor*$^{-/-}$ NK cells. In contrast, activating receptors acquired during maturation like 2B4, NKG2D or Ly49D, Ly49G2 and Ly49H were expressed at lower amounts. The percentages of cells expressing Ly49s were however similar in the presence or absence of mTOR with the exception of Ly49H (Supplementary Fig. 5b). The T-box factors Eomes and Tbet, responsible for NK cell maturation [28] were also downregulated in NK-*Mtor*$^{-/-}$ NK cells. As expected, the nutrient receptor CD71 and glucose uptake were downregulated in the absence of mTOR. CD122 and CD132, molecules constituting the IL-15Rβγc heterodimer were both halved in the absence of mTOR (Fig. 4d). The functional significance of this difference is explored below. The other markers analyzed were not changed, indicating that mTOR deletion affected selectively part of the NK gene expression program. A similar pattern was observed in the BM (Supplementary Fig. 5c).

The NKp46 promoter also drives Cre expression in IL-22 producing NCR^{+} ILC3 found in the gut. We thus investigated whether mTOR deletion affected this subset. Indeed, NKp46^{+} ILC3 cells are absent of the gut of NK-*Mtor*$^{-/-}$ animals (Supplementary Fig. 4d) pointing toward a non-redundant role of mTOR for the generation of this population.

Overall, these results demonstrate that a functional mTOR is required for the presence of mature NK cells in peripheral organs selectively affecting part of the NK gene expression program.

Optimal response to IL-15 depends on mTOR

We next tested if the absence of mature NK cells in the periphery of NK-*Mtor*$^{-/-}$ animals was a result of decreased survival, decreased generation or both. Viability of NK-*Mtor*$^{-/-}$ splenic NK cells was identical to mTOR sufficient cells for the CD11b^{lo} and DP subsets and only mildly decreased for the mature CD27^{lo} subset (Fig. 5a). Moreover, acute mTOR deletion in Mtor$^{lox/lox}$ NK cells treated *in vitro* with the cell-permeable TATCre and transferred back *in vivo* did not impair their grafting capacity compared to cotransfered TATCre treated Mtor$^{WT/WT}$ cells (Supplementary Fig. 6a). Thus, viability decrease probably only plays a minor role in the defect observed. The CD11b^{lo} to DP transition is preceded in the BM by a proliferation phase [29]. mTOR deletion resulted in a 3-fold decrease in the percentage of proliferating cells as determined by BrdU incorporation (Fig. 5b) or Ki67 staining (Supplementary Fig. 6b). This is likely to profoundly affect the output from the BM and block subsequent NK cell differentiation. NK cell proliferation is controlled by IL-15. As noted above, NK-*Mtor*$^{-/-}$ NK cells have around half the amount of surface β (CD122) and γ (CD132) chains for the IL-15 receptor than do WT cells (Fig. 5c and Supplementary Fig. 6c). This translated into a decreased steady state amount of pSTAT5 in the BM (Fig. 5c and Supplementary Fig. 6c). In support of a role of mTOR in the maintenance of an optimal IL-15R expression, acute mTOR deletion induced by TATCre treatment led to a consistent decrease in CD122 surface expression (Supplementary Fig. 6d). Quantification of STAT5 phosphorylation in response to *in vitro* treatment with increasing

Europe PMC Funders Author Manuscripts

Europe PMC Funders Author Manuscripts

concentration of IL-15 led to the finding that NK-*Mtor*$^{-/-}$ cells properly sense low IL-15 concentrations and only become defective at concentrations able to induce proliferation (Fig. 5d and data not shown). This suggests that IL-15R is limiting when NK-*Mtor*$^{-/-}$ NK cells are exposed to an IL-15-rich environment dictating NK cell proliferation.

Overall, these results show that mTOR deficiency has a strong impact on NK cell proliferation in the BM due to direct and indirect effects through the regulation of IL15R expression. The maturation block observed in NK-*Mtor*$^{-/-}$ NK cells is likely a consequence of this proliferation defect.

NK cell activation is defective in the absence of mTOR

To test the role of mTOR in NK cell activation, we treated CD45.2 *Mtor*$^{lox/lox}$ and CD45.1 *Mtor*$^{WT/WT}$ splenocytes *in vitro* with the cell-permeable TATCre and transferred them *in vivo* into double positive CD45.1/CD45.2 hosts. Two days later, hosts were injected or not with poly(I:C) and spleens harvested 18 hours later. Phosflow demonstrated a consequent decrease in mTOR catalytic activity, resulting from mTOR deletion (Fig. 6a). Cell size increase resulting from NK cell activation was suppressed in mTOR deficient cells suggesting an incapacity of these cells to upregulate metabolism (Fig. 6b). Consistent with this idea, upregulation of the nutrient receptors CD71 and CD98 as well as 2-NBDG uptake was blunted as well as CD69 up-regulation (Fig. 6c). This is coherent with the known role of mTOR in metabolic regulation and nutrient uptake.

Regarding effector functions, poly(I:C) induced GzmB expression was halved in NK cells rendered deficient in mTOR (Fig. 6d). Similar results were obtained when we compared the poly(I:C) response of NK-*Mtor*$^{WT/WT}$ and NK-*Mtor*$^{-/-}$ animals (Supplementary Fig. 7a to c). We also monitored CD11b^{lo} NK cell degranulation and IFNγ secretion following *in vitro* stimulation with a combination of IL-12 and IL-18 or plate-bound agonistic antibody specific for the activating NK cell receptor NKp46, NK1.1 and Ly49D. These tests were conducted on resting or poly(I:C) pre-activated splenic NK cells. As expected, poly(I:C) pre-activation led to a three-fold increase in the proportion of cells degranulating in response to cytokines or antibodies (Supplementary Fig. 7d). In contrast, if basal degranulation was fairly normal in the absence of mTOR, poly(I:C) stimulation was unable to enhance it (Supplementary Fig. 7d). IFN-γ production followed a similar pattern when we looked at response to NK activating receptor stimulation. However, IL-12+18 stimulation drove normal IFN-γ responses, in terms of percentage (Supplementary Fig. 7d) and quantity per cell (data not shown). The latter finding demonstrates that NK-*Mtor*$^{-/-}$ cells are reactive to IL-12+IL-18 and not generally insensitive to stimuli.

In order to assess the impact of mTOR deficiency on a more physiological NK cell response, we infected NK-*Mtor*$^{WT/WT}$ and NK-*Mtor*$^{-/-}$ animals with MCMV. During MCMV infection, it is well-described that early NK cell activation is mediated by a combination of different cytokines[30] while later during the infection, the interaction between Ly49H and the microbial encoded protein m157 drives the proliferation and sustains the activation of Ly49H^{+} NK cells[31]. We measured proliferation, GzmB, IFN-γ, KLRG1 and CCL3 expression as well as degranulation of Ly49H^{+} and Ly49H^{-} NK cell subsets during the cytokine-driven (early) and m157/Ly49H-dependent (late) phases of the response. The

Europe PMC Funders Author Manuscripts

Europe PMC Funders Author Manuscripts

cytokine-driven phase of the response was severely impaired in terms of GzmB (Fig. 6e, middle) and CCL3 (Supplementary Fig. 7e, middle) expression as well as degranulation (Supplementary Fig. 7e, right), which is in agreement with data in figure 6D and S7C and D. In contrast, we confirmed that IFNγ secretion was unaffected by mTOR deficiency (Fig. 6e, right). Surprisingly, at day 6,5 mTOR deficient Ly49H$^+$ NK cells expanded 12-fold. This proliferation was however weaker than that of control NK cells (25 fold) and the number of mTOR deficient Ly49H$^+$ NK cells never reached that of WT Ly49H$^+$ NK cells. Interestingly, the induction of KLRG1 NK cells following MCMV infection was impaired in the absence of mTOR in both Ly49H$^+$ and Ly49H$^-$ subsets (Fig. 7e).

Overall these results demonstrate that mTOR deficiency profoundly impairs early cytokine-driven NK cell activation at multiple levels. In contrast, m157-Ly49H$^+$ induced proliferation is partly mTOR independent. The latter result correlates with the previously reported independence on IL-15 of Ly49H-mediated NK cell proliferation during MCMV infection[32].

mTOR inhibition abrogates inflammation induced priming

The above results suggest that mTOR deficiency can impact NK cell cytotoxicity. To test this hypothesis further and to eliminate confounding developmental effects, we first stimulated WT NK cells using IL-15 *in vitro* and acutely inhibited mTOR using pharmacological inhibitors: Rapamycin, a clinically used mTORC1 inhibitor[33], or 2 preclinically-tested ATP-competitors inhibiting mTORC1 and mTORC2: Ku-0063794 and PP242[34,35]. To evaluate inhibitor efficacy, we measured S6 phosphorylation. All 3 inhibitors consistently impaired pS6 and GzmB increase in response to IL-15, Ku-0063794 and PP242 showing higher potency (Fig. 7a). As Rapamycin is a clinically used inhibitor, we fed mice for 2 days with an orally administered form of Rapamycin prior to poly(I:C) treatment to test whether *in vivo* inhibition could be achieved. Indeed, treatment with the drug resulted in decreased pS6 and GzmB content (Fig. 7b). Rapamycin treatment did not seem to impact IL-15 trans-presentation to NK cells since pAkt S473 and CD69 up-regulation were normal (Supplementary Fig. 8a and b). We then directly tested whether Rapamycin treatment impaired NK cell reactivity toward missing-self targets. To this aim, we transferred a mix of WT and NK-sensitive MHC class I negative (*B2m* KO) target cells into control or poly(I:C) injected mice, previously orally fed or not with Rapamycin. Target cell rejection is significantly less efficient in Rapamycin treated animals stressing out the importance of mTOR activity in NK cell function (Fig 7c). Rapamycin is used in a number of therapeutic settings. We thus thought it important to test whether human NK cell priming was sensitive to mTOR inhibitors. To answer this question, human NK cells were stimulated *in vitro* with IL-2 in the presence of mTOR inhibitors and S6 phosphorylation and GzmB content were measured. IL-2 induced a clear increase in pS6, which, as expected, was suppressed by mTOR pharmacological inhibitors (Fig. 7d). mTOR inhibitors also prevented IL-2-induced GzmB expression (Fig. 7d) with little effect on Perforin (Supplementary Fig. 8c). These results show that, as in mouse, the mTOR pathway controls human NK cell cytotoxicity downstream IL-15R.

Europe PMC Funders Author Manuscripts

Europe PMC Funders Author Manuscripts

Overall, these results show that mTOR activity in NK cells is inhibited *in vitro* and *in vivo* by pharmacological inhibitors and that this inhibition results in decreased NK cell priming and cytolytic functionality.

Discussion

mTOR is an integrator of various extracellular cues [21]. Among all the signals tested *in vitro*, we found IL-15 and IL-18 +/− IL-12 were the only inducers of mTORC1 and mTORC2 activity in NK cells. In contrast, none of the other homeostatic cytokines or agonistic antibodies known to stimulate NK activating receptors had any effect on mTOR activity. This is unexpected since T cell receptor (TCR) plus CD28 ligation is a potent inducer of mTOR activity [36-38] and the pathways induced by NK activating receptor or TCR plus CD28 ligation are remarkably similar [39]. This *in vitro* finding was corroborated by the fact that following MCMV infection, Ly49H dependent responses were less affected than cytokine dependent response of the Ly49H$^-$ NK cell subset. It thus seems that the Ly49H dependent signal is able to bypass the need for mTOR signaling. Proliferation in particular is still consequent in the absence of mTOR. It is known that Ly49H-mediated proliferation can be independent of IL-15[32] which may explain the non-essential role of mTOR in this context. We hypothesize that Ly49H-dependent signals compensate in part for the lack of IL-15 responsiveness to induce NK cell proliferation. In CD8 T cells, several pathways converge at the level of ribosomal protein S6 phosphorylation to control metabolic signaling[40]. In particular MEK-ERK MAPK pathways contribute to S6 phosphorylation which might compensate for mTOR deficiency in NK cells[40].

How mTOR is activated downstream of IL-15 receptor in NK cells remains also unsolved. To date, mTORC2 mode of activation remains elusive but involves PI3K [41]. Concerning mTORC1, the exact sequence of events leading to its activation in T cells and in particular the involvement of PI3K signal is still debated[42]. However, an intriguing fact is the observation that p110γ/δ double deficient[43] or p110δ deficient[44,45] NK cells have a partially convergent phenotype with NK-*Mtor*$^{-/-}$ NK cells, albeit milder. Indeed, defect in PI3K signaling prevents final NK cell maturation [43] and impairs their response toward NK activating receptors [43-45]. The importance of PI3K for NK cell responsiveness to IL-15 was not tested in these studies. This suggests that mTOR activity is partly but not exclusively controlled by PI3K in NK cells.

IL-15 is a pivotal cytokine controlling multiple aspects of NK cell biology. We demonstrate that IL-15 controls both steady state and activation induced mTOR activity in NK cells. Several groups have reported that different amounts of IL-15 bioavailability trigger a multiplicity of effects on NK cells, ranging from induction of cell survival at low concentration, to activation and proliferation at higher concentrations[14,16,25]. The molecular basis of this phenomenon is however unclear. Here, we show that the Jak-STAT5 and mTOR pathways are activated by different doses of IL-15. We thus hypothesize that the different outcomes resulting from varying strength of IL-15 signaling are due to the relative involvement of these two pathways. STAT5 when triggered alone would control cell viability as shown by others [17,46] while activation of both pathways together would be

Europe PMC Funders Author Manuscripts

Europe PMC Funders Author Manuscripts

responsible for proliferation and activation. This model is supported by the fact that mTOR deletion marginally affects NK cell viability but impairs their proliferation and activation.

The phenotype of NK-*Mtor*$^{-/-}$ NK cells correlates well with NK cell metabolic requirements during development and activation. Indeed, NK cell differentiation is associated to the onset of cell quiescence as shown by the decrease in cell size and glucose uptake concomitant with a loss of the transmembrane nutrient receptors CD71 and CD98. These changes are transcriptionally regulated, since we observed a selective enrichment of metabolic terms associated with decreased cell cycle and increased catabolism along differentiation. We propose that mTOR deletion blocks subsequent differentiation by blocking early steps of NK cell development associated with proliferation. In this respect, the developmental defect observed in NK cells from mice under caloric restriction might be due to a partial mTOR inhibition [47]. Moreover, it became recently evident that metabolic regulators control effector T cell function [18]. We made a similar observation in NK cells since mTOR deletion greatly reduces their ability to be activated in response to poly(I:C) treatment. Indeed, despite normal upregulation of early markers like CD69, NK-*Mtor*$^{-/-}$ NK cells have impaired expression of GzmA and GzmB. Moreover, responses of mTOR deficient NK cells to NK activating receptors triggering and in particular degranulation is completely insensitive to poly(I:C) injection. Therefore, mTOR controls a key checkpoint for NK cell activation. How mTOR mediates these effects remains the field of future investigations. We found that IL-15 mediated activation induced a strong increase in glycolysis and respiration. These essential bioenergetic pathways likely support increasing energetic demand associated with cellular activation and proliferation. Moreover, mTOR is known to increase both qualitatively and quantitatively mRNA translation through inactivation of 4EBP1[48]. This could be particularly relevant for NK cells that contain high levels of untranslated mRNA for effector molecules such as granzyme B or perforin[25]. Finally, mTOR also regulates cytoskeleton rearrangements through PKCα[49], which could be important for cell-cell interactions required for proper NK cell activation. For example, abundant literature describes the role of IL-15 transpresentation by dendritic cells to NK cells during inflammation[50].

Rapamycin is a clinically approved mTORC1 inhibitor, mainly used in renal transplantation, in the treatment of renal and breast cancers and in the treatment of affectations like Tuberous sclerosis [33]. Several Rapamycin derivatives and ATP-competitive active site inhibitors of mTOR are also developed and clinically tested. More recently, mTOR has been viewed as a potential target for anti-aging therapy and some of these inhibitors could be used on healthy patients [33]. Given our results in mice, we tested the effect of some of these inhibitors on NK cell cytotoxicity. Treatments resulted in inhibition of GzmB induction following IL-15 stimulation *in vitro*. *In vivo* treatment with Sirolimus (a clinical form of Rapamycin) decreased noticeably NK cell cytotoxicity toward missing-self targets. Remarkably, these results could be translated in human since activation of NK cells from healthy donors was inhibited by mTOR inhibitors underlining the evolutionarily conserved role of this kinase in the control of NK cell cytotoxicity. These results could have broad implications in the design of therapies targeting mTOR.

In summary, these findings reveal that mTOR is an essential part of the IL-15 signaling pathway in NK cells and controls two key checkpoints of their biology: development in the

Europe PMC Funders Author Manuscripts

Europe PMC Funders Author Manuscripts

bone marrow and activation in the periphery. Moreover, we expand to NK cells the well-documented role of Rapamycin as an immunosuppressant of adaptive immunity. Given the frequent therapeutic use of mTOR inhibitors, these findings may have direct clinical implications.

Online methods

Mice

This study was carried out in strict accordance with the French recommendations in the Guide for the ethical evaluation of experiments using laboratory animals and the European guidelines 86/609/CEE. All experimental studies were approved by the bioethic local committee CECCAPP. Wild-type C57BL/6 mice were purchased from Charles River Laboratories (L'Arbresle). *NKp46*^{iCre} [27] were crossed with *Mtor*$^{lox/lox}$ mice [26] and bred in our animal house. Female mice 8 to 24 week old were used unless specified. For some experiments, mice were injected i.p. with 150μg Polyinosinic:polycytidylic acid (poly(I:C), Invivogen) and sacrificed 4 or 18h later as indicated. For MCMV infections, mice were infected intraperitoneally with 50 000 PFU of the MCMV Smith strain.

Flow cytometry

Single cell suspension of BM, blood, spleen and liver were obtained and stained. Intracellular stainings for E4BP4, T-bet, Eomes, Ki67, granzyme A and granzyme B were performed using Foxp3 Fixation/Permeabilization Concentrate and Diluent. Intracellular stainings for mTOR were performed using Cytofix/Cytoperm (BD-Bioscience). Intracellular stainings for phosphorylated proteins were done using Lyse/Fix and PermIII buffers (BD-bioscience). BrdU incorporation was measured using a kit (Becton-Dickinson), 2mg BrdU per mouse were injected ip on day 0 and 1. Mice were sacrificed on day 2. Cell viability was measured using Annexin V/7-AAD staining (BD-bioscience). Flow cytometry was carried out on a FACS Canto, a FACS LSR II, a FACS Fortessa (Becton-Dickinson) or a Navios 5Beckman Coulter). Data were analysed using FlowJo (Treestar).

Cell culture and stimulation

Splenic lymphocytes were prepared and cultured with cytokines (rmIL-15 100ng/ml; rmIL-12 25ng/ml; rmIL-18 5ng/ml; hTGFb1 5ng/ml; rmIL-7 20ng/ml from R&D Systems or rmIFNb 100U/ml from PBL), or on antibody coated plates (anti-NKp46, anti-NK1.1, anti-Ly49D, anti-NKG2D, anti-Ly49C/I, anti-NKG2A, all at 10μg/ml) and Golgi-stop (BD-Biosciences) in the presence of anti-CD107a for 4h. Surface and intracellular stainings were then performed and IFN-γ production as well as CD107a exposure was measured by flow cytometry.

Human whole blood samples from healthy donors were collected by venous puncture in heparin containing vials. PBMCs were then isolated by Ficoll gradient centrifugation and stimulated for 36h at 37°C using 1.000UI/mL rhIL-2 in the presence or absence of mTOR inhibitors. Intracellular stainings for pS6, GzmB and Perforin were performed using the FoxP3 Fixation/Permeabilization Concentrate and Diluent (eBioscience).

Europe PMC Funders Author Manuscripts

Europe PMC Funders Author Manuscripts

Rapamycin (Sigma-Aldrich; 10 to 100nM), PP242 (Sigma-Aldrich; 1μM) and Ku-0063794 (Stemgent; 3μM) were used.

Treatment with Tat-Cre and adoptive transfers

A 1:1 mixture of spleen cells from CD45.1 C57BL/6 and NKp46^{iCre} × Mtor$^{lox/lox}$ CD45.2 mice was treated with Tat-Cre (50μg/ml, Excellgene) *in vitro* in medium without serum for 45 minutes at 37°C. They were then washed and injected retro-orbitally into recipient CD45.1 × CD45.2 C57BL/6 mice (1-2 × 10^7/mouse). 2 days later, some recipient mice were injected with poly(I:C) while other were left as controls. All mice were sacrificed the day after and transferred cells were analyzed in the spleen.

Antibodies

The following mAbs from eBioscience or BD-biosciences or Biolegend were used: anti-CD19 (ebio1D3), anti-CD3 (145-2C11), anti-NK1.1 (PK136), anti NKp46 (29A1.4), anti-CD11b (M1/70), anti-CD27 (LG.7F9), anti-CD122 (5H4 or TMb1), anti-CD132 (TUGh4), anti-CD127 (A7R34), anti-CD45.1 (A20), anti-CD45.2 (104), anti-CXCR3 (CXCR3-173), anti-CXCR4 (2B11), anti-CCR2 (475301), anti-Ly49EF (CM4), anti-Ly49D (4e5), anti-Ly49G2 (4D11), anti-Ly49H (3D10), anti-NKG2ACE (20d5), anti-NKG2D (CX5), anti-CD69 (H1.2F3), anti-CD71 (C2), anti-CD98 (RL388), anti-KLRG1 (2F1), anti-CD49b (DX5), anti-CD244 (ebio244f4), anti-E4BP4 (S2M-E19), anti-T-bet (ebio4B10), anti-Eomes (Dan11mag), anti-granzyme A (3G8.5), anti-granzyme B (NGZB), anti-IFN-g (XMG1), anti-CD107a (1D4B), anti-Ki67 (SolA15) and relevant isotype controls. Anti-mTOR (2983) was from Cell Signaling Technologies. For human cells, the following mAbs from Beckman Coulter, BioLegend or eBioscience were used: CD3 (UCHT1), CD56 (HLDA6), CD14 (RMO52), CD19 (HD237), GzB (GB11), Perforin (ΔG9). Antibodies against phosphorylated proteins were from BD-biosciences: pAkt S473 (M89-61), pSTAT5 (47/Stat5(pY694)) or Cell Signaling Technologies: pS6 (5316), p4EBP1 (7547), pAkt T308 (2965), pmTOR S2448 (5536) and pmTOR S2481 (2974).

IL-15 activity was neutralized *in vivo* by blocking the IL-2/IL-15Rβ subunit. Anti-IL-2Rβ mAb clone TM-b1 and control antibody (clone LTF-2) were purchased from Bio X Cell. F(ab)' was prepared using Pierce F(ab)'2 Micro Preparation Kit (Thermo Scientific). Mice were injected with 0.5 mg of F(ab)' 4h before analysis. In some experiments, mice were fed Sirolimus (Rapamune, Wyeth Europa Ltd) by oral gavage, 100μg/day for the indicated number of days. Gut cells were prepared as described in Luci et al (2009).

NK cell purification

NK cells were purified using biotinylated antibodies directed against CD3, CD19, CD5, CD24, F4/80 and Ly6G which were then recognized by anti-biotin beads (Miltenyi) before passing onto an AutoMACS (Miltenyi) using the DepleteS program.

Glucose uptake assessment

Glucose uptake was measured using 2-(N-(7-Nitrobenz-2-oxa-1,3-diazol-4-yl)Amino)-2-Deoxyglucose (2-NBDG, Invitrogen). Freshly isolated cells were resuspended in complete

Europe PMC Funders Author Manuscripts

Europe PMC Funders Author Manuscripts

medium in the presence of 100μM 2-NBDG for 10min at 37°C, they were then stained for surface markers.

Seahorse analysis

O_2 Consumption Rate (OCR) and ExtraCellular Acidification Rate (ECAR) were measured in XF media (non buffered DMEM containing 2mM Glutamine pH7.4) under basal condition and in response to Glucose 25mM, Oligomycin 1μM, FCCP 1,5M + pyruvate 1mM and Actimycin A 1μM + Rotenone 0,1μM with the XF-24 Extracellular Flux Analyzer (Seahorse Bioscience). IL-15 activated (100ng/ml) or resting NK cells were purified and plated (350 000 cells per well) in CellTak (Corning) coated Seahorse plate. After adhesion, the OCR and ECAR were analyzed in real time during 155 minutes.

In vivo cytotoxicity assay

Splenocytes from C57BL/6 or β2MKO mice were labeled respectively with CellTraceViolet (1μM) or CFSE (5μM) (both from Invitrogen), and 5–10 × 10^6 cells were transferred by i.v. injection. 14h after transfer, splenocytes were isolated and analyzed by FACS. Percentage of remaining ß2MKO cells was calculated using the following formula: % remaining cells= 100 × (number ß2MKO cells/number WT cells) at 14h/(number ß2MKO cells/number WT cells) in input mix.

GSEA Analyzes

Various sets of public expression data were used to identify genes in which expression was modulated upon NK cell differentiation or activation. To statistically test whether GeneSets were enriched in specific conditions, we performed pairwise comparisons between conditions using the gene set enrichment analysis (GSEA) method (http://www.broad.mit.edu/gsea). Enrichment were considered significant for an FDR<0.1.

Statistical analyzes

Error bars represent the standard deviation. Statistical analyzes were performed using two-tailed t-tests or non-parametric tests when appropriate. These tests were run on the Prism software (GraphPad). Levels of significance are expressed as p-values (*p<0.05, **p<0.01, ***p<0.001).

Supplementary Material

Refer to Web version on PubMed Central for supplementary material.

Acknowledgements

Authors thank the Plateau de Biologie Expérimentale de la Souris, and the flow cytometry facility of the SFR Biosciences Gerland and of IRCAN (the Cytomed platform funded by the CG06, INSERM and FEDER). The T. W. lab is supported by the FINOVI foundation, Agence Nationale de la Recherche (ANR JC sphinks), European Research council (ERC-Stg 281025), Institut National de la Santé et de la Recherche Médicale (INSERM), Centre National de la Recherche Scientifique (CNRS), Université Claude Bernard Lyon1, ENS de Lyon. The E.G. Lab is supported by the “Ligue contre le Cancer” (“équipe labelisée”). E.V laboratory is supported by the European Research Council (THINK Advanced Grant), by Equipe Labellisée La Ligue and by institutional grants from INSERM, CNRS, and Aix-Marseille University to CIML.

Europe PMC Funders Author Manuscripts

Europe PMC Funders Author Manuscripts

References

1. Vivier E, Tomasello E, Baratin M, Walzer T, Ugolini S. Functions of natural killer cells. Nat. Immunol. 2008; 9:503–510. [PubMed: 18425107]
2. Spits H, et al. Innate lymphoid cells--a proposal for uniform nomenclature. Nat. Rev. Immunol. 2013; 13:145–149. [PubMed: 23348417]
3. Walzer T, et al. Natural killer cell trafficking in vivo requires a dedicated sphingosine 1-phosphate receptor. Nat. Immunol. 2007; 8:1337–1344. [PubMed: 17965716]
4. Luci C, et al. Influence of the transcription factor RORgammat on the development of NKp46+ cell populations in gut and skin. Nat. Immunol. 2009; 10:75–82. [PubMed: 19029904]
5. Sanos SL, et al. RORγt and commensal microflora are required for the differentiation of mucosal interleukin 22-producing NKp46+ cells. Nat. Immunol. 2009; 10:83–91. [PubMed: 19029903]
6. Satoh-Takayama N, et al. Microbial Flora Drives Interleukin 22 Production in Intestinal NKp46+ Cells that Provide Innate Mucosal Immune Defense. Immunity. 2008; 29:958–970. [PubMed: 19084435]
7. Chiossone L, et al. Maturation of mouse NK cells is a 4-stage developmental program. Blood. 2009; 113:5488–5496. [PubMed: 19234143]
8. Hayakawa Y, Smyth MJ. CD27 dissects mature NK cells into two subsets with distinct responsiveness and migratory capacity. J Immunol. 2006; 176:1517–24. [PubMed: 16424180]
9. Cooper MA. In vivo evidence for a dependence on interleukin 15 for survival of natural killer cells. Blood. 2002; 100:3633–3638. [PubMed: 12393617]
10. Kennedy MK, et al. Reversible defects in natural killer and memory CD8 T cell lineages in interleukin 15-deficient mice. J Exp Med. 2000; 191:771–80. [PubMed: 10704459]
11. Lodolce JP, et al. IL-15 receptor maintains lymphoid homeostasis by supporting lymphocyte homing and proliferation. Immunity. 1998; 9:669–76. [PubMed: 9846488]
12. Vosshenrich CAJ, et al. Roles for common cytokine receptor gamma-chain-dependent cytokines in the generation, differentiation, and maturation of NK cell precursors and peripheral NK cells in vivo. J Immunol. 2005; 174:1213–21. [PubMed: 15661875]
13. Mortier E, et al. Macrophage- and Dendritic-Cell-Derived Interleukin-15 Receptor Alpha Supports Homeostasis of Distinct CD8+ T Cell Subsets. Immunity. 2009; 31:811–822. [PubMed: 19913445]
14. Lee GA, et al. Different NK Cell Developmental Events Require Different Levels of IL-15 Trans-Presentation. J. Immunol. 2011; 187:1212–1221. [PubMed: 21715685]
15. Orr SJ, Quigley L, Mcvicar DW. In vivo expression of signaling proteins in reconstituted NK cells. J Immunol Methods. 2009; 340:158–163. [PubMed: 19028500]
16. Orr SJ, et al. Implications for Gene Therapy-Limiting Expression of IL-2R c Delineate Differences in Signaling Thresholds Required for Lymphocyte Development and Maintenance. J. Immunol. 2010; 185:1393–1403. [PubMed: 20592278]
17. Eckelhart E, et al. A novel Ncr1-Cre mouse reveals the essential role of STAT5 for NK-cell survival and development. Blood. 2011; 117:1565–1573. [PubMed: 21127177]
18. Pearce EL, Pearce EJ. Metabolic Pathways in Immune Cell Activation and Quiescence. Immunity. 2013; 38:633–643. [PubMed: 23601682]
19. Chang C-H, et al. Posttranscriptional Control of T Cell Effector Function by Aerobic Glycolysis. Cell. 2013; 153:1239–1251. [PubMed: 23746840]
20. Sinclair LV, et al. Phosphatidylinositol-3-OH kinase and nutrient-sensing mTOR pathways control T lymphocyte trafficking. Nat Immunol. 2008; 9:513–521. [PubMed: 18391955]
21. Laplante M, Sabatini DM. mTOR Signaling in Growth Control and Disease. Cell. 2012; 149:274–293. [PubMed: 22500797]
22. Magnuson B, Ekim B, Fingar DC. Regulation and function of ribosomal protein S6 kinase (S6K) within mTOR signalling networks. Biochem J. 2011; 441:1–21. [PubMed: 22168436]
23. Wang R, Green DR. Metabolic checkpoints in activated T cells. Nat. Immunol. 2012; 13:907–915. [PubMed: 22990888]

Europe PMC Funders Author Manuscripts

Europe PMC Funders Author Manuscripts

24. Baranek T, et al. Differential Responses of Immune Cells to Type I Interferon Contribute to Host Resistance to Viral Infection. Cell Host Microbe. 2012; 12:571–584. [PubMed: 23084923]
25. Fehniger TA, et al. Acquisition of murine NK cell cytotoxicity requires the translation of a pre-existing pool of granzyme B and perforin mRNAs. Immunity. 2007; 26:798–811. [PubMed: 17540585]
26. Risson V, et al. Muscle inactivation of mTOR causes metabolic and dystrophin defects leading to severe myopathy. J Cell Biol. 2009; 187:859–874. [PubMed: 20008564]
27. Narni-Mancinelli E, et al. Fate mapping analysis of lymphoid cells expressing the NKp46 cell surface receptor. Proc. Natl. Acad. Sci. U. S. A. 2011; 108:18324–18329. [PubMed: 22021440]
28. Gordon SM, et al. The Transcription Factors T-bet and Eomes Control Key Checkpoints of Natural Killer Cell Maturation. Immunity. 2012:1–13. doi:10.1016/j.immuni.2011.11.016.
29. Kim S, et al. In vivo developmental stages in murine natural killer cell maturation. Nat. Immunol. 2002; 3:523–528. [PubMed: 12006976]
30. Nguyen KB, et al. Coordinated and Distinct Roles for IFN-αβ, IL-12, and IL-15 Regulation of NK Cell Responses to Viral Infection. J. Immunol. 2002; 169:4279–4287. [PubMed: 12370359]
31. Dokun AO, et al. Specific and nonspecific NK cell activation during virus infection. Nat. Immunol. 2001; 2:951–956. [PubMed: 11550009]
32. Sun JC, Ma A, Lanier LL. Cutting Edge: IL-15-Independent NK Cell Response to Mouse Cytomegalovirus Infection. J. Immunol. 2009; 183:2911–2914. [PubMed: 19648279]
33. Johnson SC, Rabinovitch PS, Kaeberlein M. mTOR is a key modulator of ageing and age-related disease. Nature. 2013; 493:338–345. [PubMed: 23325216]
34. Feldman ME, et al. Active-site inhibitors of mTOR target rapamycin-resistant outputs of mTORC1 and mTORC2. Plos Biol. 2009; 7:e38. [PubMed: 19209957]
35. García-Martínez JM, et al. Ku-0063794 is a specific inhibitor of the mammalian target of rapamycin (mTOR). Biochem J. 2009; 421:29–42. [PubMed: 19402821]
36. Delgoffe GM, et al. The mTOR Kinase Differentially Regulates Effector and Regulatory T Cell Lineage Commitment. Immunity. 2009; 30:832–844. [PubMed: 19538929]
37. Frauwirth KA, et al. The CD28 signaling pathway regulates glucose metabolism. Immunity. 2002; 16:769–77. [PubMed: 12121659]
38. Lee K, et al. Mammalian Target of Rapamycin Protein Complex 2 Regulates Differentiation of Th1 and Th2 Cell Subsets via Distinct Signaling Pathways. Immunity. 2010; 32:743–753. [PubMed: 20620941]
39. Watzl C, Long EO. Signal transduction during activation and inhibition of natural killer cells. Curr Protoc Immunol. 2010 **Chapter 11,** Unit 11.9B.
40. Salmond RJ, Emery J, Okkenhaug K, Zamoyska R. MAPK, Phosphatidylinositol 3-Kinase, and Mammalian Target of Rapamycin Pathways Converge at the Level of Ribosomal Protein S6 Phosphorylation to Control Metabolic Signaling in CD8 T Cells. J Immunol. 2009; 183:7388–7397. [PubMed: 19917692]
41. Frias MA, et al. mSin1 is necessary for Akt/PKB phosphorylation, and its isoforms define three distinct mTORC2s. Curr. Biol. CB. 2006; 16:1865–1870. [PubMed: 16919458]
42. Finlay DK, et al. PDK1 regulation of mTOR and hypoxia-inducible factor 1 integrate metabolism and migration of CD8+ T cells. J. Exp. Med. 2012:1–28. doi:10.1084/jem.20112607. [PubMed: 22184634]
43. Tassi I, et al. p110gamma and p110delta phosphoinositide 3-kinase signaling pathways synergize to control development and functions of murine NK cells. Immunity. 2007; 27:214–27. [PubMed: 17723215]
44. Guo H, Samarakoon A, Vanhaesebroeck B, Malarkannan S. The p110 of PI3K plays a critical role in NK cell terminal maturation and cytokine/chemokine generation. J. Exp. Med. 2008; 205:2419–2435. [PubMed: 18809712]
45. Kim N, et al. The p110delta catalytic isoform of PI3K is a key player in NK-cell development and cytokine secretion. Blood. 2007; 110:3202–3208. [PubMed: 17644738]
46. Hand TW, et al. Differential effects of STAT5 and PI3K/AKT signaling on effector and memory CD8 T-cell survival. Proc. Natl. Acad. Sci. 2010; 107:16601–16606. [PubMed: 20823247]

47. Clinthorne JF, Beli E, Duriancik DM, Gardner EM. NK Cell Maturation and Function in C57BL/6 Mice Are Altered by Caloric Restriction. J. Immunol. 2013; 190:712–722. [PubMed: 23241894]

48. Thoreen CC, et al. A unifying model for mTORC1-mediated regulation of mRNA translation. Nature. 2012; 485:109–13. [PubMed: 22552098]

49. Jacinto E, et al. Mammalian TOR complex 2 controls the actin cytoskeleton and is rapamycin insensitive. Nat Cell Biol. 2004; 6:1122–1128. [PubMed: 15467718]

50. Marçais A, et al. Regulation of mouse NK cell development and function by cytokines. Front. NK Cell Biol. 2013; 4:450.

Europe PMC Funders Author Manuscripts

Europe PMC Funders Author Manuscripts

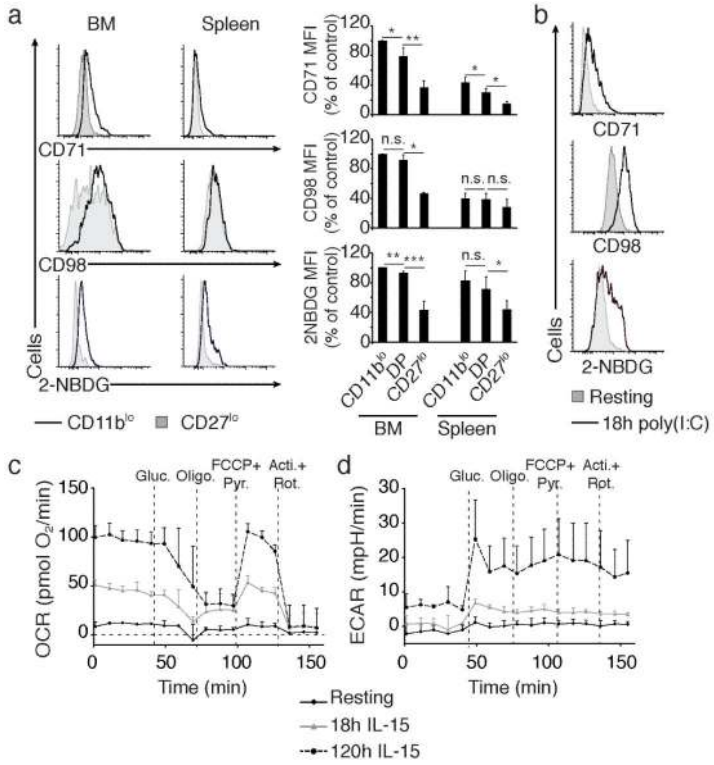

Figure 1.

NK cell metabolism is regulated developmentally and following activation (**a**) Representative flow cytometric analyses of the expression of CD71 and CD98 or the amount of 2-NBDG staining from bone marrow (BM) or splenic NK CD11b^{lo} versus CD27^{lo} subsets as indicated. The bar graph shows averaged MFI (+/− s.d.) for CD71, CD98 or 2-NBDG of BM and splenic NK cell subsets (n=4 mice in 4 independent experiments, t-test, *p<0.05, **p<0.01, ***p<0.001). MFI were normalized to the CD11b^{lo} subset in the BM. (**b**) Histograms represent CD71, CD98 and 2-NBDG expression on splenic NK cells from control injected or mice injected with poly(I:C) 18 h before, one representative experiment out of 3 is shown. (**c** and **d**) Primary NK cells were stimulated or not with IL-15 for 18 h or 120 h and NK cell metabolism was analyzed. OXPHOS (OCR for O_2 Consumption Rate) (**c**) and Aerobic Glycolysis (ECAR for ExtraCellular Acidification Rate) (**d**) were analyzed in real time after injection of Glucose 25 mM, Oligomycin 1 μM, FCCP 1.5 M + pyruvate 1 mM and Actimycin A 1 μM + Rotenone 0.1 μM as indicated. Curves represent the average of 3 independent mice performed in triplicate (2 independent experiments).

Europe PMC Funders Author Manuscripts
Europe PMC Funders Author Manuscripts

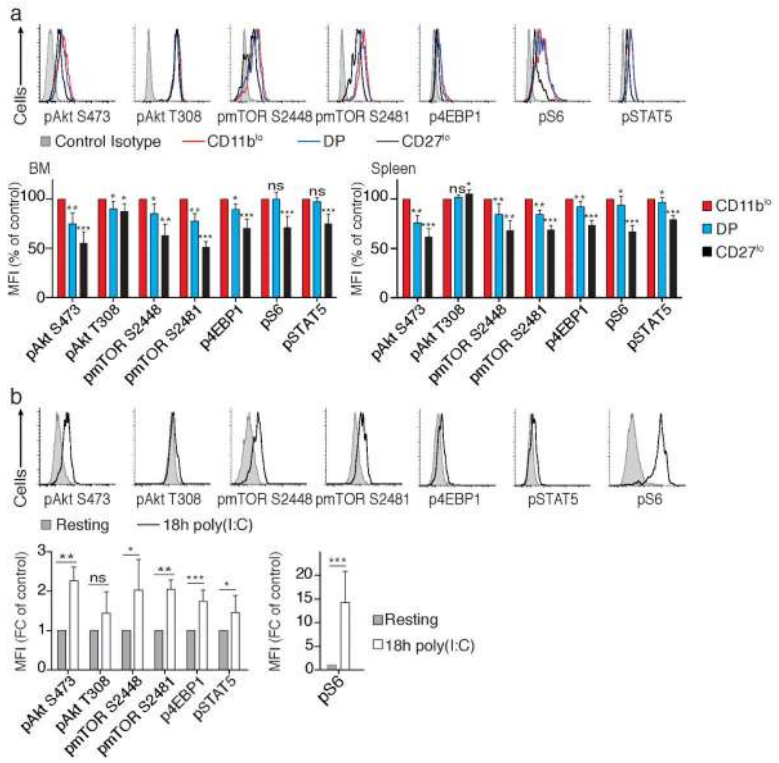

Figure 2.

mTOR activity decreases as differentiation progresses and is upregulated upon activation (**a**) Phosphorylation of different proteins in BM NK cell subsets as defined by the expression of CD27 and CD11b, one representative experiment out of 4 is shown. The bar graph shows averaged phosphoproteins MFI (+/− s.d.) of BM and splenic NK cell subsets (n=4 mice in 4 independent experiments). MFI is normalized to the CD11b^{lo} subset. (**b**) Phosphorylation of different proteins in splenic NK cells from control or mice injected with poly(I:C) 18 h before, one representative experiment out of 3 is shown. The bar graph shows averaged phosphoproteins MFI (+/− s.d.) (n=3 mice in 3 independent experiments). Fold change (FC) in MFI is obtained by normalizing the activated to the resting population. (t-test, *p<0.05, **p<0.01, ***p<0.001, ns = non significant).

Europe PMC Funders Author Manuscripts
Europe PMC Funders Author Manuscripts

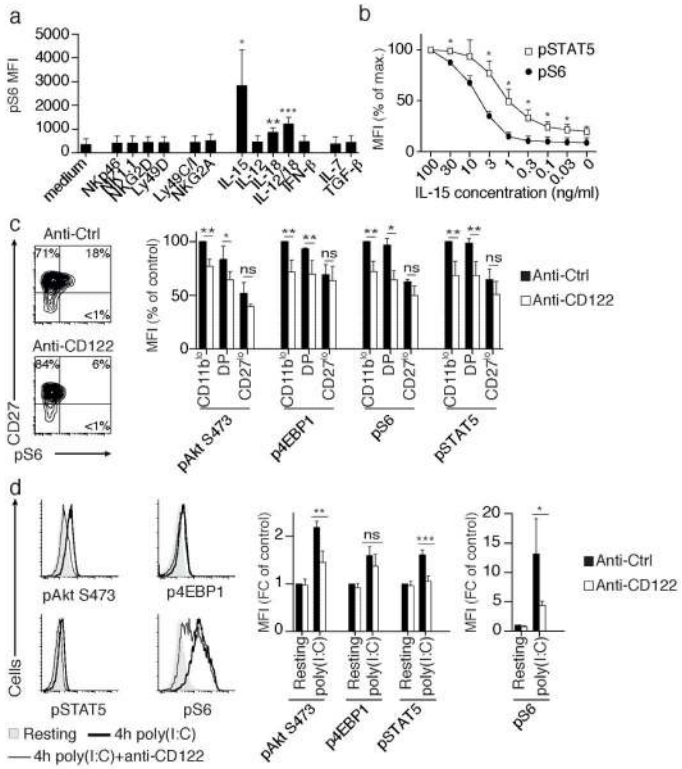

Figure 3.

mTOR activity is primarily under IL-15 control.

(**a**) Splenocytes were cultured for 1 h on plates coated with the indicated antagonistic antibodies or with the indicated cytokine. Cells were subsequently stained and the averaged MFI (+/− s.d.) of intracellular pS6 in NK cells is shown (n=4 independent experiments using 1 mouse each time). (**b**) Splenocytes were cultured with graded concentrations of IL-15 for 1 h. Cells were stained and the averaged MFI of intracellular pS6 and pSTAT5 in NK cells are given as percentage of the maximal response (+/− s.d.) (n=3 independent experiments using 1 mouse each time). (**c**) Freshly isolated BM cells of control or anti-CD122 injected mice were stained and analyzed by flow cytometry. The amount of pS6 as a function of CD27 expression in one representative experiment out of 3 is shown. The bar graph shows averaged phosphoproteins MFI of BM NK cells from control of anti-CD122 treated mice (n=3 mice in 3 independent experiments). MFI is normalized to the $CD11b^{lo}$ subset. (**d**) Histograms represent phosphorylation of different proteins in splenic NK cells from control or poly(I:C) injected mice 4 h before, with or without anti-CD122, one representative experiment out of 3 is shown. The bar graph shows averaged phosphoproteins MFI (+/− s.d.) (average of n=3 mice in 3 independent experiments). Fold change (FC) in MFI is obtained by normalizing the activated to the resting population. (t-test, *p<0.05, **p<0.01, ***p<0.001, ns = non significant).

Europe PMC Funders Author Manuscripts
Europe PMC Funders Author Manuscripts

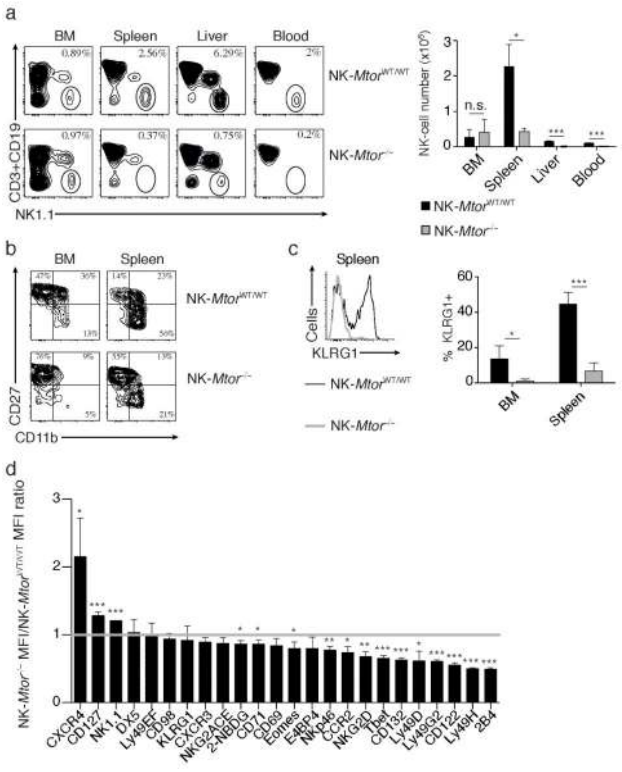

Figure 4.

mTOR controls NK cell maturation and homeostasis.

(**a**) Single cell suspension from various organs of NK-*Mtor*$^{WT/WT}$ (*NKp46*^{ICre}) and NK-*Mtor*$^{-/-}$ (*NKp46*^{ICre}*Mtor*$^{lox/lox}$) mice were stained for NK1.1, CD3 and CD19. Representative flow cytometric analyzes out of 3 experiments are shown. Cell suspensions were numerated and the number of NK cell calculated. The bar graph shows the average number (+/− s.d.) of NK cells in BM, Spleen, Liver and Blood of NK-*Mtor*$^{WT/WT}$ and NK-*Mtor*$^{-/-}$ mice (average of n=3 mice in 3 independent experiments). (**b**) Representative flow cytometric analysis showing CD27 and CD11b expression on gated NK cells from the BM and Spleen of NK-*Mtor*$^{WT/WT}$ and NK-*Mtor*$^{-/-}$ mice . More than 10 experiments showed the same profile. (**c**) Representative histograms show KLRG1 expression on splenic NK cells of NK-*Mtor*$^{WT/WT}$ and NK-*Mtor*$^{-/-}$ mice . The bar graph shows the average percentage (+/− s.d.) of KLRG1 positive cells among BM and Spleen NK cells (n=4 mice in 3 independent experiments). (**d**) MFI of the indicated marker was measured on spleen CD11b^{-} NK cells from NK-*Mtor*$^{WT/WT}$ and NK-*Mtor*$^{-/-}$ mice. The bar graph shows the average of the ratio of MFIs (+/− s.d.) NK-*Mtor*$^{-/-}$ over NK-*Mtor*$^{WT/WT}$ NK cells for each marker (n=3 mice in 3 independent experiments). The grey line indicates a ratio of 1. (t-test, *p<0.05, **p<0.01, ***p<0.001).

Europe PMC Funders Author Manuscripts
Europe PMC Funders Author Manuscripts

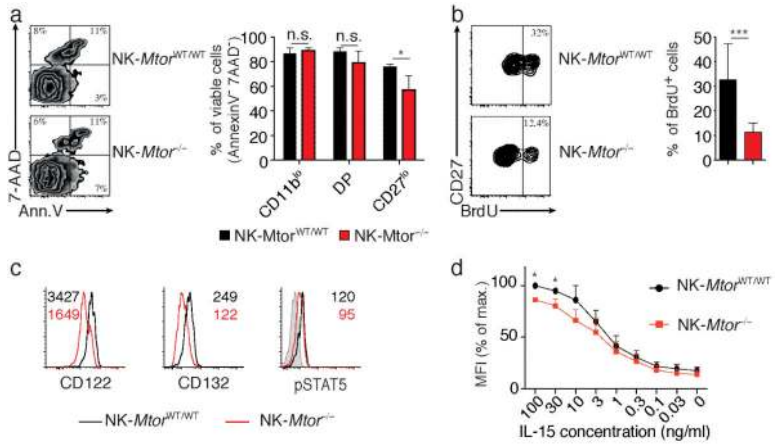

Figure 5.

mTOR is necessary for NK cell optimal fitness, proliferation in the BM and maximal response to IL-15.

(**a**) Flow cytometric analyzes show AnnexinV and 7-AAD staining of splenic NK cells from NK-*Mtor*$^{WT/WT}$ and NK-*Mtor*$^{-/-}$ mice. One representative experiment out of 3 is shown. The bar graph shows average percentages (+/− s.d.) of viable cells (AnnexinV-7-AAD-) in the different NK cell subsets from NK-*Mtor*$^{WT/WT}$ and NK-*Mtor*$^{-/-}$ mice (n=3 mice in 3 independent experiments). (**b**) Flow cytometric analyzes show BrdU staining of CD11b^{lo} subset BM NK cells from NK-*Mtor*$^{WT/WT}$ and NK-*Mtor*$^{-/-}$ mice. One representative experiment out of 3 is shown. The bar graph shows average percentages (+/− s.d.) of BrdU positive cells (n=6 mice in 3 independent experiments). (**c**) Histograms represent expression of CD122, CD132 and pSTAT5 in CD11b^{lo} BM NK cells from NK-*Mtor*$^{WT/WT}$ and NK-*Mtor*$^{-/-}$ mice. MFI values are indicated. One representative experiment out of 4 with 1 mouse in each is shown. (**d**) Splenocytes from NK-*Mtor*$^{WT/WT}$ and NK-*Mtor*$^{-/-}$ mice were cultured with graded concentrations of IL-15 for 1 h. Cells were stained and the averaged MFI (+/− s.d.) of pSTAT5 in NK cells is given as percentage of the maximal response (n=3 independent experiments using 1 mouse in each). (t-test, *p<0.05, **p<0.01, ***p<0.001, ns = non significant).

Europe PMC Funders Author Manuscripts
Europe PMC Funders Author Manuscripts

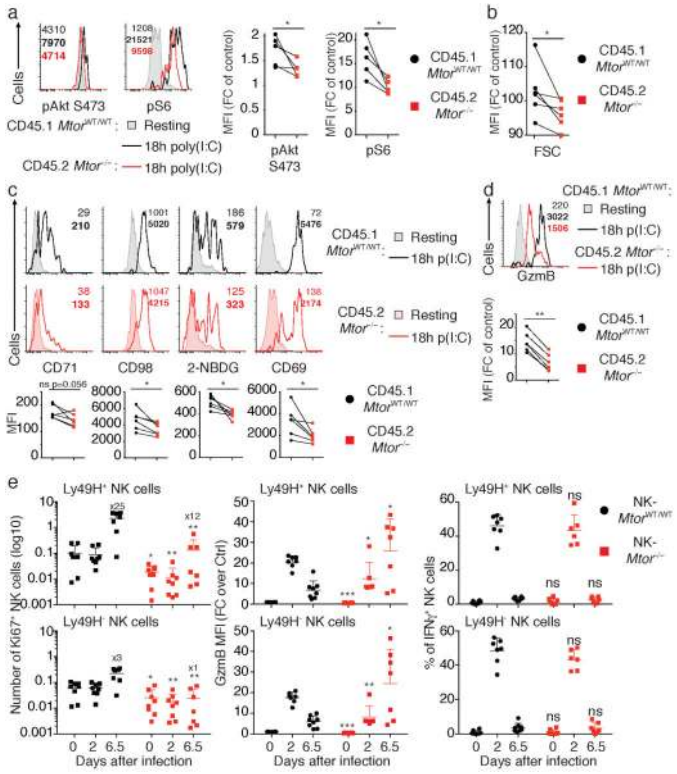

Figure 6.

Defective NK cell activation in the absence of mTOR.

(**a-d**) CD45.1 *Mtor*$^{WT/WT}$ or CD45.2 *Mtor*$^{lox/lox}$ splenocytes treated *in vitro* with TATCre were transferred into CD45.1/CD45.2 double positive hosts. 2 days later, mice were injected or not with poly(I:C). Splenic cell suspension were analyzed 18 h later by flow cytometry. (**a**) Histograms represent phosphorylation of S6 and Akt proteins (one representative experiment out of 3 (t-test, *p<0.05, **p<0.01, ***p<0.001, ns = non significant). independent experiments using 1 mouse in each), numbers indicate the MFI. The scatter plot shows phosphoproteins MFI in NK cells from poly(I:C) injected mice (n=5 mice, 3 independent experiments). MFI is normalized to the resting population. (**b**) The scatter plot shows FSC MFI in NK cells from poly(I:C) injected mice (n=6 mice, 3 independent experiments). (**c**) Histograms represent expression of CD71, CD98 and CD69 or the amount of 2-NBDG staining in one experiment out of 3, numbers indicate the MFI. The scatter plot shows MFI in NK cells from poly(I:C) injected mice (n=6 mice, 3 independent experiments). (**d**) Histograms show intracellular expression of GzmB in one representative experiment out of 3. The scatter plot shows MFI normalized to the resting population (n=5 mice, 3 independent experiments). (**a-d**) In all scatter plots, lines link the CD45.1 *Mtor*$^{WT/WT}$ and CD45.2 *Mtor*$^{-/-}$ NK cells co-transferred in the same host. (**e**) NK-*Mtor*$^{WT/WT}$ and NK-*Mtor*$^{-/-}$ mice were infected with MCMV and sacrificed at day 0, 2 or 6.5. Expression of intracellular Ki67, GzmB and IFN-γ analyzed in Ly49H^{+} and Ly49H^{-} splenic NK cell subsets. The number of Ki67^{+} NK cells as well as the GzmB MFI (normalized to non-infected mice) and the percentage of IFN-γ^{+} NK cells in each subset is shown (average +/− SD, dots represent individual mice, statistical comparisons have been made between NK-*Mtor*$^{WT/WT}$ and NK-*Mtor*$^{-/-}$ NK cells for each time point). Ki67^{+} NK

Europe PMC Funders Author Manuscripts
Europe PMC Funders Author Manuscripts

cell proliferation is indicated. Results are from more than at least 6 mice, 4 independent experiments. (t-test, *p<0.05, **p<0.01, ns = non significant).

Europe PMC Funders Author Manuscripts

Europe PMC Funders Author Manuscripts

Europe PMC Funders Author Manuscripts

Europe PMC Funders Author Manuscripts

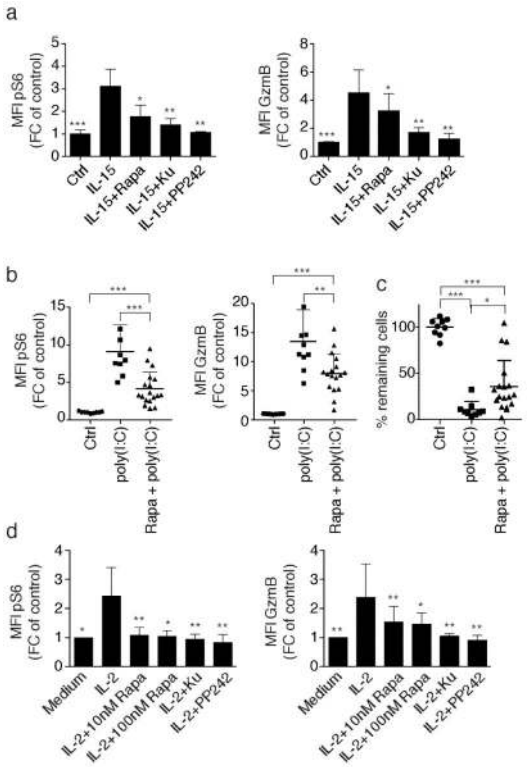

Figure 7.

Acute mTOR inhibition abrogates inflammation induced priming.

(**a**) Splenocytes were cultured for 14 h in the presence of IL-15 at 100 ng/mL with or without mTOR inhibitors as indicated. Cells were then stained and analyzed by flow cytometry. The bar graphs show the averaged MFI (+/− s.d.) for pS6 and GzmB in gated NK cells (n=5 independent experiments with 1 mouse in each). (**b**) Rapamycin treated or non-treated mice were injected with poly(I:C) and sacrificed 18h later. Splenocytes were analyzed by flow cytometry. The graphs show the averaged MFI for pS6 and GzmB in gated NK cells. Each dot represents a single mouse, bars indicate average and SD (n=9 mice in 4 independent experiments for poly(I:C) and 18 mice in 4 independent experiments for Rapa +poly(I:C)). The MFI was normalized to control non-poly(I:C) injected mice. (**c**) *In vivo* cytotoxicity toward missing-self targets was assessed as described in the Experimental Procedures section. The percentage of remaining cells was calculated and is shown. Each dot represents a single mouse, bars indicate average and SD (n=9 mice in 4 independent experiments for poly(I:C) and 18 mice in 4 independent experiments for Rapa+poly(I:C)). (**d**) Human PBMCs were cultured for 36h as indicated. Cells were then stained and analyzed by flow cytometry. The bar graphs show the averaged MFI for pS6 and GzmB in gated NK cells (n=9 individual donors in 3 independent experiments, paired t-test, *p<0.05, **p<0.01).